Available online at www.sciencedirect.com
SCIENCE DIRECT®
Journal of Solid State Chemistry 177 (2004) 4087–4092
JOURNAL OF SOLID STATE CHEMISTRY
www.elsevier.com/locate/jssc

# Pressure-induced amorphization in $Y_2(WO_4)_3$: in situ X-ray diffraction and Raman studies

S. Karmakar[a,*], S.K. Deb[a], A.K. Tyagi[b], Surinder M. Sharma[a]

[a] *Bhabha Atomic Research Centre, Synchrotron Radiation Section, Mumbai, 400 085, India*
[b] *Applied Chemistry Division, Bhabha Atomic Research Centre, Mumbai, 400 085, India*

Received 15 June 2004; received in revised form 19 July 2004; accepted 16 August 2004
Available online 7 October 2004

**Abstract**

The high-pressure behavior of $Y_2(WO_4)_3$ has been investigated at room temperature by in situ X-ray diffraction and Raman scattering measurements. Both the studies show that beyond ~3 GPa, this compound smoothly transforms from the ambient orthorhombic phase to a disordered phase. The structural modifications are found to be reversible up to ~4 GPa but become irreversible at higher pressures. Low pressures of transformation imply that these changes are intrinsic and not due to non-hydrostatic stresses. In addition, the correlation between the stability range of orthorhombic phase and counter cation size supports that this compound has a large field of negative thermal expansion in this family of compounds.


*Keywords:* High pressure; $Y_2(WO_4)_3$; X-ray diffraction; Raman scattering

## 1. Introduction

Since the discovery of negative thermal expansion (NTE) in many tungstates and molybdates [1], there have been several investigations aimed at the understanding of structural behavior of these compounds under different thermodynamic conditions. Many of these compounds display temperature and pressure-dependent phase transformations and several of these also transform to an amorphous phase at high pressures [2–7]. Several of these compounds belong to $A_2(MO_4)_3$ family of compounds (with $M = W^{6+}$ or $Mo^{6+}$ and $A$ ranging from $Al^{3+}$ to some of the heavier trivalent rare-earth cations) and have structures characterized by three-dimensional framework of corner-linked alternate $AO_6$ octahedra and $MO_4$ tetrahedra. Due to this, structural modifications, as brought about by the pressure and temperature variations, including eventual amorphization under compression, involve rotations/tilts of nearly rigid tetrahedra [8–13]. For example, $Sc_2(WO_4)_3$ transforms from the orthorhombic phase to a low-symmetry phase at ~2 GPa before an irreversible amorphization at ~4 GPa [14,15]. $Al_2(WO_4)_3$ also undergoes phase transformation from the orthorhombic phase before turning amorphous at high pressures [14,16,17]. For many of these NTE compounds, although the volume contracts upon increase in the temperature, this change may not necessarily be negative along all the three crystallographic axes. However, Yittrium tungstate [$Y_2(WO_4)_3$], which crystallizes in orthorhombic $Sc_2(WO_4)_3$ type structure (space group *Pnca*), is one such compound which shows large NTE along all the three crystallographic axes. Moreover, this NTE behavior exists over a wide temperature range (15–1373 K), without undergoing any phase transformation. In addition, this material has the highest negative value of volume thermal expansion coefficient ($\alpha_v = -20.9 \times 10^{-6}/^{\circ}C$) [8]. It would be interesting to find whether the high-pressure behavior of $Y_2(WO_4)_3$ is any different from other members of this family. Therefore, we have now carried out high-pressure

*Corresponding author. Fax: +91-22-2550-5151.
*E-mail address:* sdak@magnum.barc.ernet.in (S. Karmakar).

0022-4596/$ - see front matter © 2004 Elsevier Inc. All rights reserved.
doi:10.1016/j.jssc.2004.08.020

Raman and X-ray diffraction measurements, which are presented here.

## 2. Experimental

Appropriate amounts of $Y_2O_3$ and $WO_3$ (both 99.9% pure) were mixed thoroughly, palletized and heated at 900 °C for 30 h, with an intermittent grinding and palletizing after ~15 h. The product obtained after this heat treatment, slightly yellowish in color, was again thoroughly ground, mixed, repelletized and heated at 1100 °C for 4 h. All the heat treatments were carried out in the static air. The resulting white compound was characterized by powder X-ray diffraction to be phase-pure $Y_2W_3O_{12}$ (JC-PDS card no. 15-0447). In situ high-pressure X-ray diffraction experiments were performed by angle dispersive X-ray diffraction system using the graphite monochromatized Mo-$K\alpha$ X-rays ($\lambda = 0.7107$ Å) from a Rigaku rotating anode X-ray generator and mar345 imaging plate area detector. For these studies, the powdered $Y_2(WO_4)_3$ sample was loaded in a gasket hole (~140 μm diameter) of Mao–Bell kind of diamond anvil cell. To avoid hydration, we heated the material upto ~800 °C in the furnace and loaded the compound in the cell immediately after removal from the furnace. Secondly, the material was kept under a vacuum of $\sim 10^{-3}$ Torr for about 1 h and the compound was loaded immediately after taking it out of vacuum. In both the cases our results were identical. Dry methanol:ethanol (4:1) mixture was used as a pressure transmitting fluid and a small ruby chip (~20 μm) for pressure calibration [18]. The incident X-ray beam was collimated to ~100 μm and the distance between the sample and the imaging plate was kept at ~140 mm. At each pressure, the data were collected for at least 8 h and these experiments were carried out up to a hydrostatic pressure of 8.0 GPa. The two-dimensional diffraction images recorded on the image plate were integrated to get the diffraction profiles using FIT2D software [19]. For Raman measurements, 514.5 nm line of an Ar ion laser was used as the excitation source, which was incident at the sample at an angle of 45°. For modes higher than 200 $cm^{-1}$, pressure-dependent Raman spectra were obtained with a single stage spectrograph (Jobin–Yvon SPEX HR460) equipped with a supernotch filter and liquid nitrogen cooled CCD detection system. The spectrograph was calibrated using reference neon lamps and by the plasma lines from Ar ion laser. For Raman spectra in the low-frequency region (20–200 $cm^{-1}$), the excitation source was still 514.5 nm line of Ar ion laser, but the data were recorded using a scanning 750 mm double grating monochromator, coupled with a Hammamatsu R943 photomultiplier tube and computer-controlled photon counting system. The entrance slit of the monochromator was ~250 μm to keep low instrumental broadening (~2.5 $cm^{-1}$). All the Raman spectra were recorded up to a pressure of 11 GPa.

## 3. Results and discussion

### 3.1. X-ray diffraction measurements

Fig. 1(a) shows the X-ray diffraction profiles of $Y_2(WO_4)_3$ in the $2\theta$ range of 5–19° and up to 8 GPa. At ambient conditions, the diffraction profile can be fully indexed with the space group *Pnca*. The profile fitting of the data was performed by Le-Bail method using GSAS program [20]. For this, the starting structural parameters are taken from Ref. [8]. The refined cell parameters at ambient condition are found to be $a = 9.95(2)$ Å, $b = 13.92(3)$ Å, $c = 10.08(2)$ Å, which compare well with the reported values of Forster et al. [8] as obtained from neutron diffraction data viz., $a = 9.99372$ Å, $b = 13.9593$ Å, $c = 10.0838$ Å. Almost all the pressure-induced changes observed in the diffraction profiles are found to be reversible up to a pressure of 4.4 GPa as shown in Fig. 1(b). However, the unloading of pressure from 8 GPa shows irreversible degradation of the diffraction signal. The pressure dependence of the cell parameters up to ~4.4 GPa is shown in Fig. 2(a). All the diffraction peaks broaden with pressure and the inset Fig. 2(a) shows the change in width of one of the Bragg peaks (111) with pressure. The observed smooth variation of the lattice parameters implies that this compound does not undergo any phase transition up to ~4 GPa, though beyond ~2.5 GPa we observe an increased peak broadening as well as loss of diffraction signal. Fig. 2(b) shows the pressure–volume data up to 4.4 GPa along with the fits to Birch–Murnaghan (BM) equation of state [21]. If we restrict the fitting to the data prior to line broadening, i.e., up to ~2.5 GPa, we get $B = 27$ GPa and $B' = 2$. However, if we extend the analysis to ~ 4.4 GPa, we get $B = 24.2$ GPa, $B' = 6.7$. We note here that the smaller value of $B'$ is consistent with the analysis of Sikka [22] who showed that the NTE materials should have low $B'$. In addition, our low-pressure value of $B'$ is similar to what has been observed for $NbOPO_4$ [23].

As mentioned above, signal/background ratio starts deteriorating beyond ~3 GPa and is partly due to the increased line broadening at higher pressures. This implies that at around this pressure some kind of atomic positional disorder sets in, as the increased line broadening cannot be ascribed to the non-hydrostatic stresses at these low pressures. Moreover, this disorder increases with pressure and at ~8 GPa, essentially two broad diffraction peaks persist suggesting that the phase is highly disordered. Moreover, as mentioned earlier, these

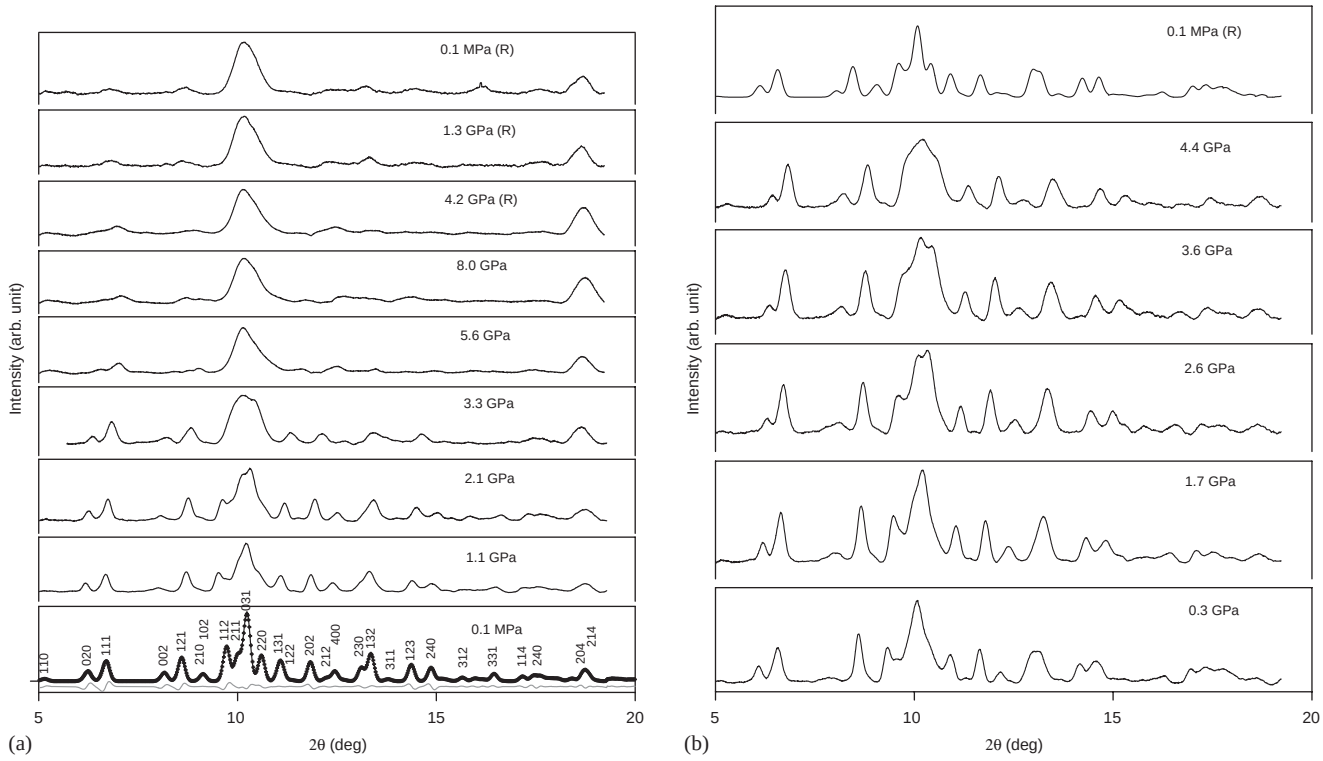


Fig. 1. (a) X-ray diffraction patterns of $Y_2(WO_4)_3$ at different pressures. At ambient conditions, the fitted profile as well as difference plot is also shown [(+) observed intensities, and (—) profile fit, difference plot is shown at the bottom]. R represents the diffraction patterns as the pressure is released from 8 GPa. (b) X-ray diffraction patterns of $Y_2(WO_4)_3$ up to 4.4 GPa and after release from this pressure.

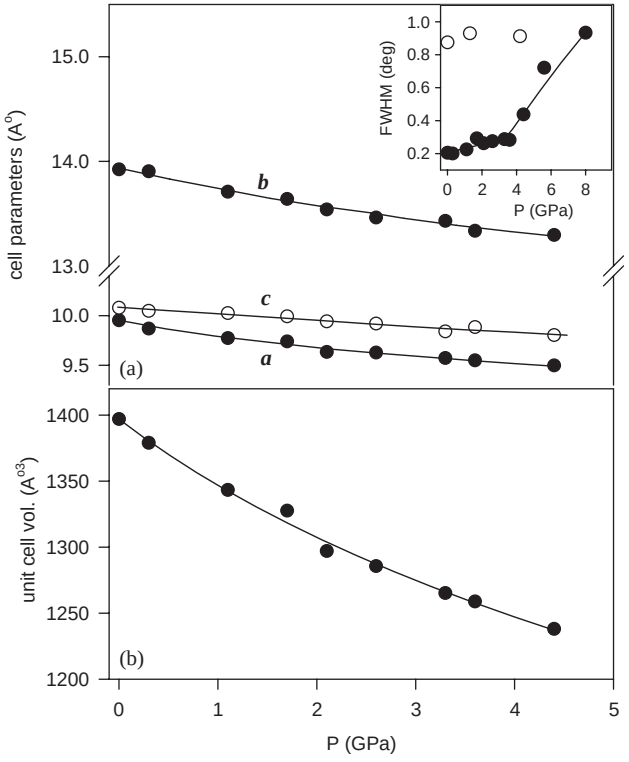


Fig. 2. (a) Variation of lattice parameters and unit cell volume as a function of pressure. The solid lines are to guide the eye. (b) Pressure–volume data have been fitted with the BM equation of state (—). Inset shows the broadening of the (111) Bragg peak with pressure. (●) Increasing pressure, and (○) releasing pressure.

changes are irreversible if $Y_2(WO_4)_3$ is compressed up to ~8 GPa.

### 3.2. Raman measurements

Fig. 3 shows Raman active lattice modes at 71, 81 and 115 $cm^{-1}$ for various pressures. At ~5.9 GPa, these modes become quite weak and disappear upon further increase of pressure. For the Raman active vibrational modes higher than ~200 $cm^{-1}$, the changes observed with pressure are shown in Fig. 4. In analogy with the Raman spectra of several tungstates of NTE group, the strong modes centered at 1016, 998 and 954 $cm^{-1}$ are assigned to the symmetric stretching of $WO_4$ tetrahedra and modes at 847 and 800 $cm^{-1}$ are taken to represent the asymmetric stretching [6]. The Raman active modes at 376 and 455 $cm^{-1}$ are assigned to the $WO_4$ symmetric and asymmetric bendings, respectively. Above 5.7 GPa, all the modes become increasingly weak and broad. At this pressure the Raman peaks are centered approximately at ~400, 870 and 980 $cm^{-1}$ implying the persistence of $WO_4$ tetrahedra. At ~11 GPa, the only visible modes are highly broadened symmetric stretch of tetrahedra. In fact, at a pressure higher than ~6 GPa, the features of our Raman spectra are very similar to the $WO_4$ Raman modes observed at 3.5 GPa in amorphous $ZrW_2O_8$ [24]. The pressure-induced variations of these Raman modes are shown in Fig. 5. Absence of any

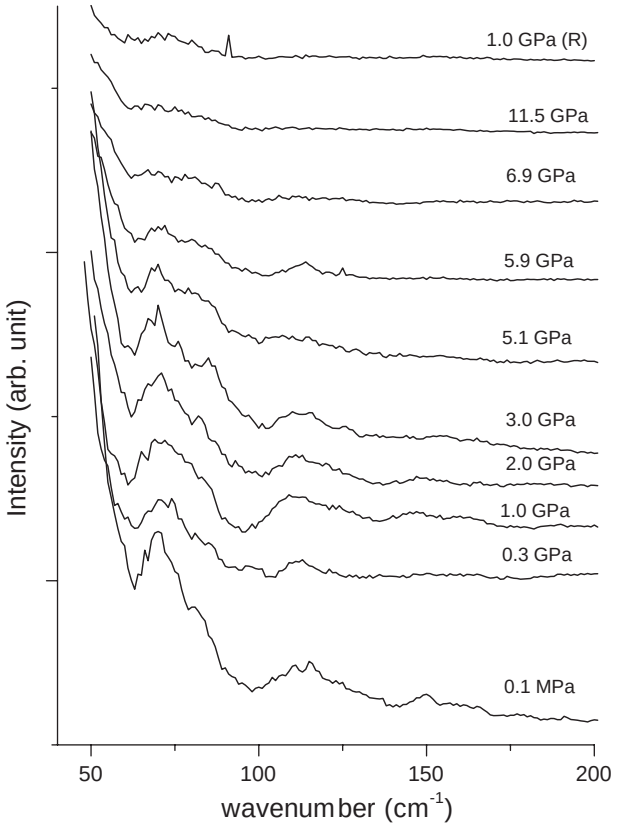


Fig. 3. Low-frequency Raman lattice modes observed at various pressures.

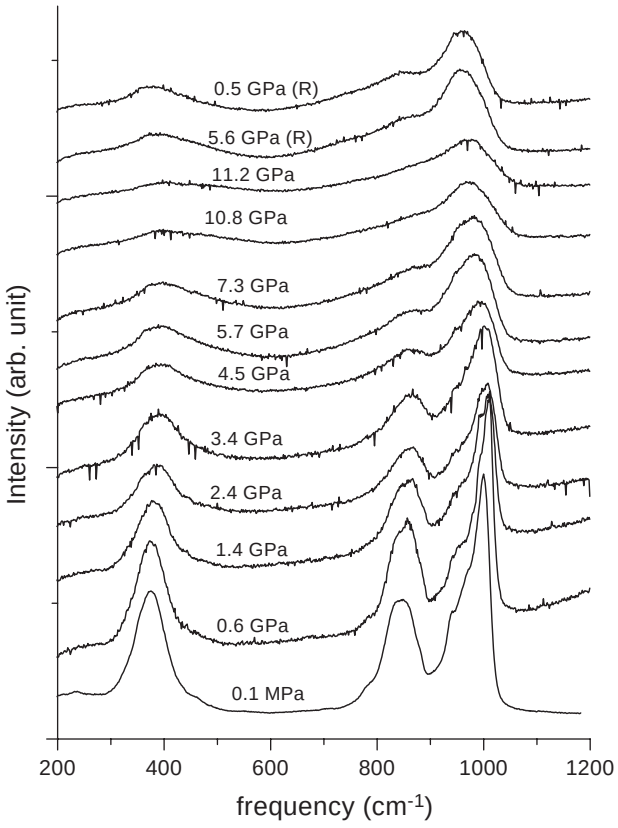


Fig. 4. High-frequency Raman internal modes observed at various pressures.

splitting of modes, or vanishing of any mode or any substantial change in slope indicates lack of any structural phase transformation, in agreement with the X-ray diffraction results. Except the symmetric stretch modes, all the modes stiffen with pressure. A similar softening of the symmetric stretch modes has also been observed in $Zr(MoO_4)_2$ [3] and in $Sc_2(MoO_4)_3$ [6]. While the complete softening of any mode leads to a structural phase transformation, the softening of the modes by a few tens of $cm^{-1}$ (by 11 GPa), as seen here, implies a small reduction in the restoring force and, may be, also a slightly larger bond length. Gross implications of our Raman results are that beyond ~6 GPa, $Y_2W_3O_{12}$ starts becoming progressively disordered while still retaining $WO_4$ tetrahedral nature. The Raman results at 11.2 GPa, suggest an amorphous state. Upon release of pressure from 11 GPa, the modes remain broad indicating the irreversible nature of the structural evolution into a disordered state. These results are in agreement with our X-ray diffraction results. And, as in the present case the pressure of emergence of disorder is much lower than the pressure of solidification of the pressure transmitting fluid, it cannot be ascribed to the onset of non-hydrostatic stresses. As mentioned earlier, similar results have also been observed in $Sc_2(WO_4)_3$ and $Al_2(WO_4)_3$.

As in most of the corner-linked structures [13], in the NTE $[A_2(MO_4)_3]$ compounds the $A$–O–$M$ bond bending is the easiest form of deformation. Thus as the lattice parameters of these compounds decrease with pressure, the $A$–O–$M$ linkage starts bending. As a consequence, the increased repulsive energy due to reducing non-bonded contacts leads to distortions of the polyhedra [10,13,22,25]. However, this variation has to compete with the crystal–crystal structural phase transitions [27]. It is well known that if a compound is kinetically frustrated to undergo a phase transition to the equilibrium form, the metastable amorphous phase becomes a preferred state [13,26]. This is clearly reflected in a correlation between the pressure of transformation and the limiting values of the non-bonded atomic distances [13,26]. Thus in some favorable cases, such as $Sc_2(WO_4)_3$ and $Al_2(WO_4)_3$ [14,16], the approach of limiting distances brings about the structural phase transformations [27], while in others, such as $Lu_2(WO_4)_3$ [7] and $Y_2(WO_4)_3$, the structure becomes amorphous. Though the pressure-dependent fractional coordinates are not available in the present case, we speculate that the onset of amorphization at ~6 GPa is quite likely to be due to the approach of limiting distance between some non-bonded (probably O–O) atoms [22,26].

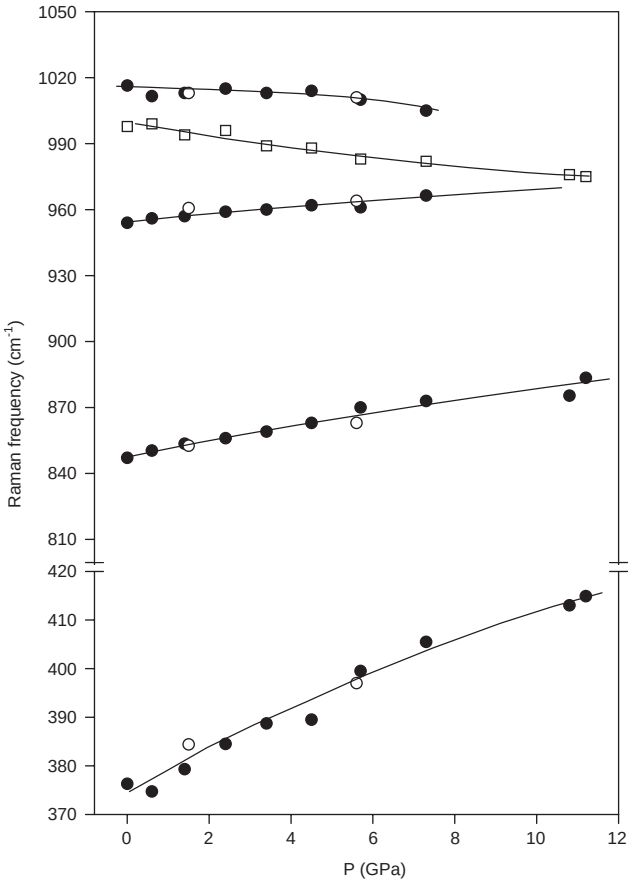


Fig. 5. Variation of internal Raman mode frequencies as a function of pressure.

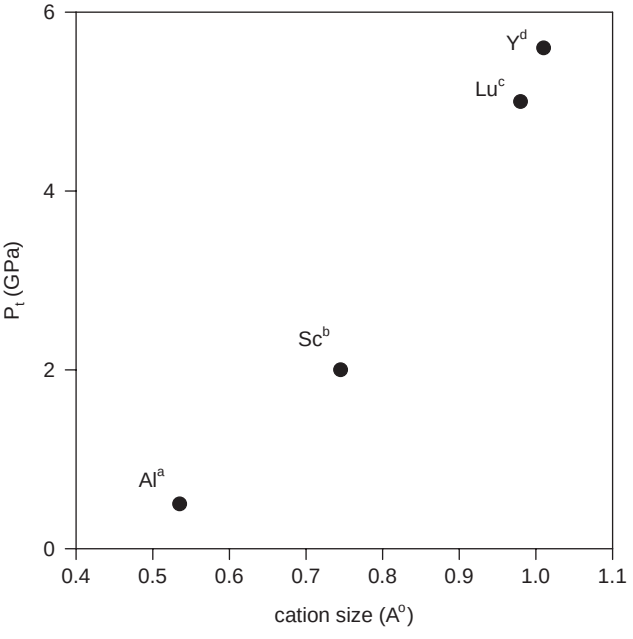


Fig. 6. Variation of the transformation pressure [at which the compounds transform from orthorhombic phase to either another crystalline phase ((a) Refs. [14,16,17], (b) Refs. [14,15]) or to an amorphous structure ((c) Ref. [7]; (d) present work)] with the cation size.

Fig. 6 shows the variation of the pressure of transformation ($P_t$) (from orthorhombic to another crystalline or amorphous phase) with the cation size. As the existence of NTE is closely related to the orthorhombic phase in this family of compounds, this figure implies that larger the counter cation size, higher the maximum pressure up to which the system can have NTE before transformation to a structure which may not show NTE. It has also been suggested that larger the counter cation size, more facile is the rocking of polyhedra, and in turn higher is the magnitude of the NTE [28]. Therefore, $Y_2(WO_4)_3$ may be one of the most useful compounds for tailoring NTE for composites.

## 4. Conclusion

Our high-pressure X-ray diffraction and Raman studies on $Y_2(WO_4)_3$ reveal that this compound monotonically and systematically evolves towards an amorphous phase beyond ~4–6 GPa. The emergence of the disordered phase at low pressures implies that the non-hydrostatic stresses do not play a vital role in these structural changes for this compound as in several other members of this family. Correlation between the stability range and counter cation size implies that this compound may have the largest field of stability in this family of compounds.

## References

[1] J.S.O. Evans, T.A. Mary, A.W. Sleight, J. Solid State Chem. 133 (1997) 580.
[2] B. Chen, D.V.S. Muthu, Z.X. Lu, A.W. Sleight, M.B. Kruger, Phys. Rev. B 64 (2001) 214111.
[3] D.V.S. Muthu, B. Chen, J.M. Wrobel, A.M. Krogh Andersen, S. Carlson, M.B. Kruger, Phys. Rev. B 65 (2002) 064101.
[4] R.A. Secco, H. Liu, N. Imanaka, G. Adachi, M.D. Rutter, J. Phys. Chem. Solid 63 (2002) 425.
[5] V. Dmitriev, V. Sinitsyn, R. Dilanian, D. Machon, A. Kuznetsov, E. Ponyatovsky, G. Lucazeau, H.P. Weber, J. Phys. Chem. Solid 64 (2003) 307.
[6] W. Paraguassu, M. Maczka, A.G. Souza Filho, P.T.C. Freire, J.M. Filho, F.E.A. Melo, L. Macalik, L. Gerward, J.S. Olsen, A. Waskowska, H. Hanuza, Phys. Rev. B 69 (2004) 094111.
[7] H. Liu, R.A. Secco, N. Imanaka, G. Adachi, Solid State Commun. 121 (2002) 177.
[8] P.M. Forster, A.W. Sleight, Int. J. Inorg. Mater. 1 (1999) 123; D.A. Woodcock, P. Lightfoot, C. Ritter, J. Solid State Chem. 149 (2000) 92.
[9] J.S.O. Evans, T.A. Mary, A.W. Sleight, Physica B 241 (1998) 311.
[10] J.Z. Tao, A.W. Sleight, J. Solid State Chem. 173 (2003) 442.
[11] A.K. Arora, R. Nithya, T. Yagi, N. Miyajima, T.A. Mary, Solid State Commun. 129 (2004) 9.
[12] J.D. Jorgensen, Z. Hu, S. Teslic, D.N. Argyriou, S. Short, J.S.O. Evans, A.W. Sleight, Phys. Rev. B 59 (1999) 215.
[13] S.M. Sharma, S.K. Sikka, Prog. Mater. Sci. 40 (1996) 1.

[14] N. Garg, C. Murli, T. Bhattacharya, S. Karmakar, A.K. Tyagi, S.M. Sharma, Solid State Phys. (India) 44 (2001) 39 (S.L. Chaplot, P.S.R. Krishna, T. Sakuntala (Eds.), Narosa Publishing House, New Delhi).
[15] R.A. Secco, H. Liu, N. Imanaka, G. Adachi, J. Mater. Sci. Lett. 20 (2001) 1339.
[16] M. Maczka, W. Paraguassu, A.G. Souza Filho, P.T.C. Freire, J. MendesFilho, F.E.A. Melo, J. Hanuza, J. Solid State Chem. 177 (2004) 2002.
[17] G.D. Mukherjee, S.N. Acharya, A.K. Tyagi, S.N. Vaidya, J. Phys. Chem. Solid 64 (2003) 611.
[18] R.A. Forman, G.J. Piermarini, J.D. Barnett, S. Block, Science 176 (1972) 284.
[19] A.P. Hammersley, S.O. Svensson, M. Hanfland, A.N. Fitch, D. Hauserman, High Pressure Res. 14 (1996) 235.
[20] A.C. Larson, R.B. Von Dreele, GSAS: general structure analysis system, Los Alamos National Laboratory, LAUR Publication, 1998.
[21] F.D. Murnaghan, Proc. Natl. Acad. Sci. USA 30 (1944) 244.
[22] S.K. Sikka, J. Phys.: Condens. Matter 16 (2004) S1033.
[23] G.D. Mukherjee, V. Vijaykumar, B.K. Godwal, S.N. Acharya, A.K. Tyagi, A. Lausi, E. Busetto, Elettra Highlights (2002–2003) 28.
[24] C.A. Perottani, J.A.H. da Jornada, Science 280 (1998) 886.
[25] R.J. Speedy, J. Phys.: Condens. Matter 8 (1996) 10907.
[26] S.K. Sikka, S.M. Sharma, Curr. Sci. 63 (1992) 317.
[27] S.K. Sikka, S.M. Sharma, R. Chidambaram, in: S.C. Schimdt, J.W. Shaner, G.A. Samara, M. Ross (Eds.), High Pressure Science and Technology, AIP Press, New York, 1994, p. 213.
[28] P.M. Forster, A. Yokochi, A.W. Sleight, J. Solid State Chem. 140 (1998) 157.